ACS Infectious Diseases

pubs.acs.org/journal/aidcbc

Article

Heterologous Protein Expression Favors the Formation of Protein Aggregates in Persister and Viable but Nonculturable Bacteria

Olivia Goode,[#] Ashley Smith,[#] Urszula Łapińska, Rosemary Bamford, Zehra Kahveci, Georgina Glover, Erin Attrill, Alice Carr, Jeremy Metz, and Stefano Pagliara*

Cite This: https://doi.org/10.1021/acsinfecdis.1c00154

Read Online

ACCESS | Metrics & More | Article Recommendations | Supporting Information

ABSTRACT: Environmental and intracellular stresses can perturb protein homeostasis and trigger the formation and accumulation of protein aggregates. It has been recently suggested that the level of protein aggregates accumulated in bacteria correlates with the frequency of persister and viable but nonculturable cells that transiently survive treatment with multiple antibiotics. However, these findings have often been obtained employing fluorescent reporter strains. This enforced heterologous protein expression facilitates the visualization of protein aggregates but could also trigger the formation and accumulation of protein aggregates. Using microfluidics-based single-cell microscopy and a library of green fluorescent protein reporter strains, we show that heterologous protein expression favors the formation of protein aggregates. We found that persister and viable but nonculturable bacteria surviving treatment with antibiotics are more likely to contain protein aggregates and downregulate the expression of heterologous proteins. Our data also suggest that such aggregates are more basic with respect to the rest of the cell. These findings provide evidence for a strong link between heterologous protein expression, protein aggregation, intracellular pH, and phenotypic survival to antibiotics, suggesting that antibiotic treatments against persister and viable but nonculturable cells could be developed by modulating protein aggregation and pH regulation.

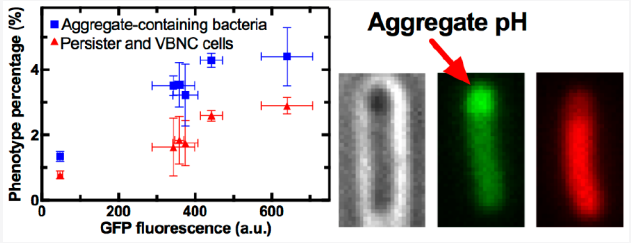

KEYWORDS: *persisters, viable but nonculturable cells, protein aggregation, antimicrobial resistance, microfluidics, heterologous expression*

Persister cells are small subsets, within a clonal bacterial population, able to survive exposure to otherwise lethal doses of antibiotics and to resume growth after antibiotic removal.[1] Viable but nonculturable (VBNC) cells also constitute small subpopulations capable of surviving antibiotic challenges but might regrow only if specific conditions, in terms, for example, of temperature and nutrients, are met.[2−4] Moreover, recent work suggests that viable but nonculturable and persister cells describe the same dormant phenotype[5−8] and that these subpopulations can be responsible for the recalcitrance of chronic infections.[9,10] Several molecular mechanisms can underlie the formation of persister and viable but nonculturable cells,[7,11] including toxin−antitoxin modules,[12] ribosome dimerization,[13] inactivation of antibiotic targets,[14] or reduced intracellular antibiotic concentration.[15] Recently, it has been suggested also that the accumulation of protein aggregates in stationary-phase bacteria contributes to the formation of persister and VBNC cells.[6,16,17]

Multicomponent protein aggregates initiate as small soluble oligomers that can grow into microscopically observable insoluble structures containing unfolded and misfolded proteins.[18] Protein aggregation occurs as a consequence of perturbations in proteostasis due to cellular and environmental factors[19] such as heat shock,[20] oxidative stress,[21] nutrient starvation,[16] protein overexpression,[22] or cellular aging.[23] Fluorescence microscopy studies have demonstrated that protein aggregates typically localize at the bacterial poles,[23,24] possibly due to the fact that bacterial nucleoids prevent unfolded and misfolded proteins from being able to diffuse freely around the cellular space, particularly as protein aggregates increase in size.[25]

Protein aggregates have been reported to provide functional benefits, despite their cellular toxicity.[22] For instance, the surface protein A induces aggregation and increases biofilm formation in *Staphylococcus aureus*.[26] The sporulation protein TasA forms oligomeric aggregates with antibacterial properties that provide *Bacillus subtilis* with a competitive advantage during colonization.[27] Furthermore, it has been suggested that the presence of protein aggregates also benefits bacteria by providing protection from antibiotics.[6,16,17] These studies often employed fluorescent reporter strains that facilitate the visualization of protein aggregates.[23,25] However, this enforced heterologous protein expression could promote the accumu-

Received: March 25, 2021

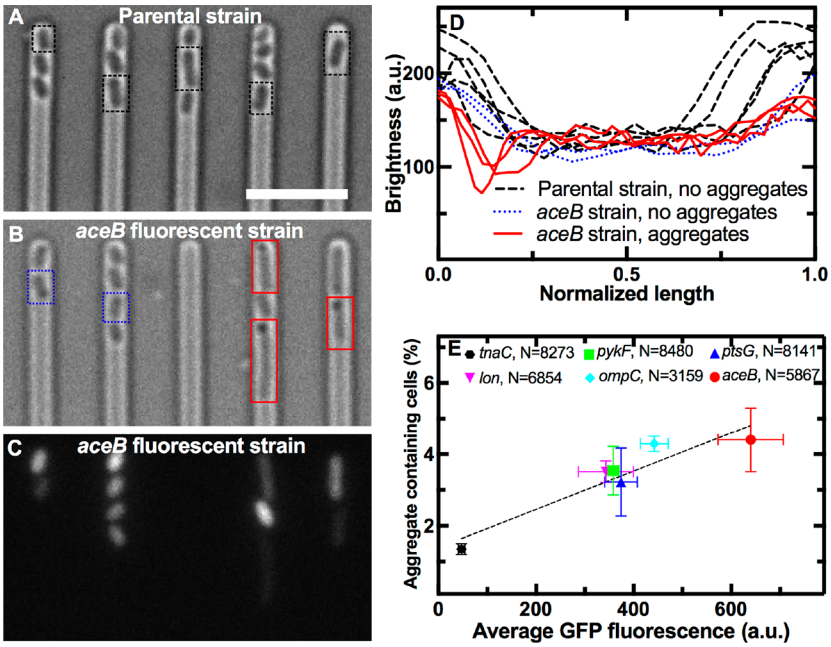

Figure 1. Heterologous protein expression favors protein aggregation. (A) Microfluidics-based bright-field live-cell image of stationary phase *E. coli* BW25113 (parental strain) with no detectable protein aggregates, five representative cells are highlighted by black dashed rectangles. Scale bar: 5 μm. (B) Microfluidics-based bright-field live-cell image of stationary phase*E. coli aceB* reporter strain with protein aggregates detectable in the cells highlighted by solid red rectangles; two representative cells without detectable protein aggregates are highlighted by blue dotted rectangles. (C) Fluorescence image reporting GFP expression from each individual cell in (B). (D) Brightness profile along the length of five representative parental strain bacteria (black dashed lines), two representative *aceB* strain bacteria without aggregates (blue dotted lines), and two representative *aceB* strain bacteria with aggregates (red solid lines) displaying significant depth in brightness in proximity of the bacterial poles. (E) Correlation between the average percentage of aggregate-containing bacteria in each reporter strain and the corresponding average GFP fluorescence of each fluorescent strain (r Pearson coefficient of 0.94, **). All images and data were obtained after 17 h of growth in LB medium before injection in the microfluidic mother machine device. Symbols and error bars are the mean and standard error of the mean of thousands of single-cell measurements performed in biological triplicate (N = 8273, 8480, 8141, 6854, 3159, and 5867 individual cells for the *tnaC*, *pykF*, *ptsG*, *lon*, *ompC*, and *aceB* reporter strains, respectively).

lation of protein aggregates due to either (i) the self-aggregating tendency of some fluorescent fusion proteins[20] or (ii) the burden imposed on the bacteria by the demand of producing exogenous proteins[22] which might overload the protein control system including chaperones and proteases. Moreover, high amounts of protein aggregates can be toxic for bacteria and can indicate cell death.[28]

In this study, we set out to determine whether the level of intracellular protein aggregation and the frequency of persister and viable but nonculturable cells can be controlled by manipulating the level of heterologous protein expression in *E. coli*. We used microfluidics-based single-cell microscopy[8,29,30] to investigate protein aggregation and phenotypic response to three antibiotics, ampicillin, gentamicin, and ciprofloxacin, in six different *E. coli* transcriptional reporter strains.[31] Each of the reporter strains has green fluorescence protein (GFP) fused to a promoter in a low-copy plasmid. Using fluorescent reporter strains for *tnaC*, *pykF*, *ptsG*, *lon*, *aceB*, and *ompC*, that collectively span 3 orders of magnitude in transcript reads in stationary phase *E. coli*,[32] we found that the percentage of aggregate-containing cells increased with the level of GFP expression. Moreover, cells containing protein aggregates before antibiotic treatment were more likely to survive exposure to ampicillin, gentamicin, or ciprofloxacin as persisters or viable but nonculturable cells. We considered bacteria to be viable but nonculturable if after 3 h antibiotic treatment and 21 h exposure to antibiotic-free medium they did not stain with propidium iodide, expressed GFP, and did not divide within our experimental time frame. However, it is conceivable that these cells could start dividing if exposed to nutrients for longer periods of time.[5,33] Furthermore, our data suggest that before antibiotic exposure persisters, that germinated after a 3 h antibiotic treatment at 25× minimum inhibitory concentration (MIC), and viable but nonculturable bacteria are more likely to contain protein aggregates. Our microscopy images also suggest that such aggregates are more basic with respect to the rest of the cell, although further studies will need to be carried out to determine whether this alkalinization causes the formation of persister and VBNC cells. Taken together, these findings strengthen the link between the accumulation of protein aggregates and phenotypic survival to antibiotics and demonstrate that heterologous protein expression can be used to manipulate both the extent of protein aggregation and the frequency of persisters and viable but nonculturable cells.

RESULTS

Heterologous Protein Expression Favors Protein Aggregation. In order to phenotype cells according to the presence or absence of protein aggregates, we combined time-lapse microscopy with the microfluidic mother machine device whose fabrication and handling has been previously reported.[8,34] This device, made of polydimethylsiloxane (PDMS), is equipped with an array of dead-end microfluidic channels with width and height of 1.5 μm and a length of 25 μm. Because *E. coli* BW25113 are rod-shaped bacteria with a

https://doi.org/10.1021/acsinfecdis.1c00154
ACS Infect. Dis. XXXX, XXX, XXX−XXX

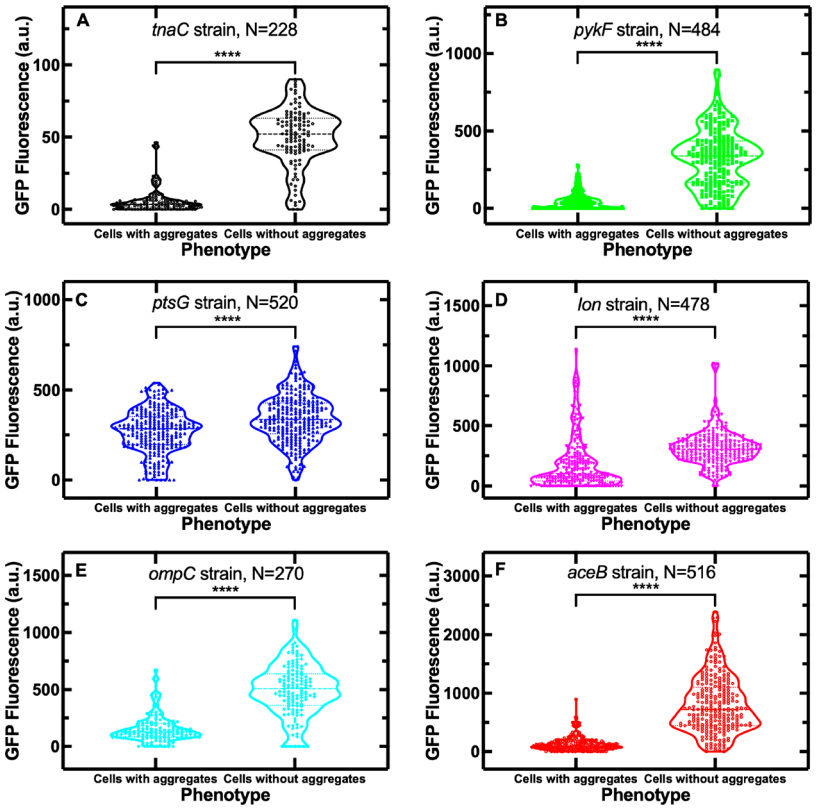

Figure 2. Aggregate-containing cells downregulate the expression of heterologous proteins. GFP fluorescence in individual stationary-phase *E. coli* bacteria with or without detectable aggregates from a (A) *tnaC*, (B) *pykF*, (C) *ptsG*, (D) *lon*, (E) *ompC*, and (F) *aceB* fluorescent reporter strain. Each data point is the GFP fluorescence value for an individual bacterium. *N* denotes the sum of the number of data points for the two phenotypes for each strain collated from biological triplicate. These data points were collected from each aggregate-containing cell for each strain and from an equal number (*N*/2) of cells without aggregates randomly selected from the whole population of cells without aggregates. **** *p*-value <0.0001.

typical width and height of less than 1 μm, each channel accommodates between 1 and 5 bacteria disposed in a single file (Figure 1A). This allows tracking of each single bacterium over time and, crucially for this work, distinguishing between cells that lack or contain protein aggregates (Figure 1A,B,D, Methods, and ref 8). In order to sustain bacterial growth, these channels are connected to a main microchamber (25 and 100 μm in height and width, respectively) continuously supplied with fresh Lysogeny broth (LB).

Despite imaging 5620 individual bacteria, we did not observe microscopic protein aggregates in stationary-phase *E. coli* BW25113 after 17 h of bulk growth in LB medium (Figure 1A and D) and in the absence of external stressors, such as heat shock or exposure to antibiotics. Although these results are consistent with previous reports,[6,20] it is also conceivable that small protein aggregates are present in stationary-phase *E. coli* but do not reach sizes which allow them to be visible under bright-field or phase contrast microscopy. Therefore, in order to validate our experimental approach we used a Δ*dnaK E. coli* strain lacking the molecular chaperone DnaK that participates in protein disaggregation in cooperation with IbpAB and ClpB.[16] By imaging 1056 individual bacteria, we found a significantly higher percentage (27.9 ± 3.4%) of aggregate containing cells compared to the *E. coli* BW25113 parental strain (Figure S1), confirming the suitability of our experimental approach in detecting the presence of protein aggregates.

Next, we investigated the presence of protein aggregates in *E. coli* BW25113 transcriptional reporter strains[31] expressing heterologous GFP. Each reporter strain has GFP fused to a promoter in a low-copy plasmid. We chose the following promoters: *tnaC*, *pykF*, *ptsG*, *lon*, *aceB*, and *ompC*; since collectively these strains span 3 orders of magnitude in transcript reads in stationary phase *E. coli*,[32] thus allowing us to determine the impact of heterologous GFP expression on protein aggregation. Furthermore, some of these genes have been previously associated with survival to antibiotics. Specifically, *tnaC* is the precursor of the *tna* operon that catabolizes tryptophan into pyruvate, ammonia, and indole, and has been linked to antibiotic persistence.[8,35−37] *pykF* is a pyruvate kinase and has been linked to bacterial adaptation into different growth phenotypes upon nutrient starvation.[38] *ptsG* is a glucose transporter which has been linked to heterogeneity in cellular metabolism.[39] *lon* is a protease whose involvement in persistence has been the center of some debate.[40] *aceB* is involved in the glyoxylate shunt during growth on acetate,[38] which has previously been linked with changes in phenotypic heterogeneity.[32,39] *ompC* is one of the major outer membrane porins that allow β-lactams, such as ampicillin, to diffuse into the cell.[41] Imaging a total of 40,774 individual bacteria from these six strains, we found that microscopic protein aggregates were clearly detectable in all the fluorescent reporter strains investigated after 17 h of growth in LB medium (Figure 1B and D). However, such aggregates were detectable only in a subset of each fluorescent strain population (Figure 1B and D). Therefore, for each strain we measured the average percentage of cells displaying detectable aggregates from biological triplicates. Moreover,

https://doi.org/10.1021/acsinfecdis.1c00154
ACS Infect. Dis. XXXX, XXX, XXX−XXX

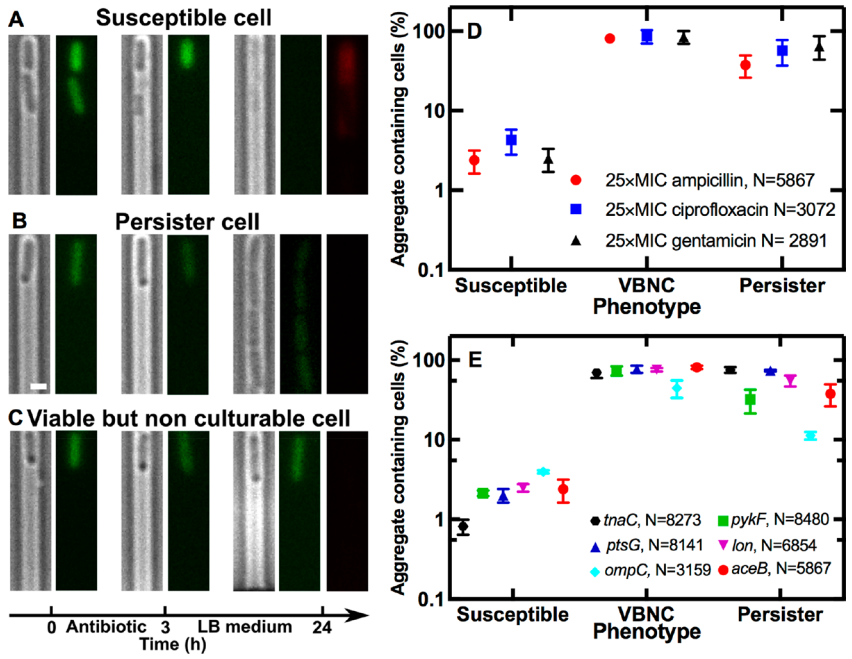

Figure 3. Presence of protein aggregates correlate with survival to antibiotic treatment. Microfluidics-based bright-field live-cell images and corresponding fluorescence images of (A) a susceptible, (B) a persister, and (C) a viable but nonculturable cell before (t = 0) and after antibiotic treatment (t = 3 h) and after a 21 h regrowth period in LB medium (t = 24 h). Images were acquired for an *E. coli aceB* reporter strain injected in the mother machine in stationary phase prior to treatment with ampicillin. At t = 24 h, a propidium iodide staining was carried out to detect dead bacteria with compromised membranes, rightmost image set. Scale bar: 1 μm. (D) Percentage of aggregate-containing cells before antibiotic treatment for subpopulations of *aceB E. coli* reporter strain cells that are susceptible, persister, or viable but nonculturable after treatment with ampicillin (circles), ciprofloxacin (squares), or gentamicin (triangles) at 25 × their minimum inhibitory concentration. Symbols and error bars are the mean and standard error of the mean of thousands of single-cell measurements performed in biological triplicate (N = 5867, 3072, and 2891 for ampicillin, ciprofloxacin, and gentamicin treatment, respectively). (E) Percentage of aggregate-containing cells before antibiotic treatment for subpopulations of *tnaC* (hexagons), *pykF* (squares), *ptsG* (upward triangles), *lon* (downward triangles), *ompC* (diamonds), and *aceB* (circles) reporter strains cells that are susceptible, persister or viable but nonculturable after treatment with ampicillin at 25× its minimum inhibitory concentration. Symbols and error bars are the mean and the standard error of the mean of thousands of single-cell measurements performed in biological triplicate (N = 8273, 8480, 8141, 6854, 3159, and 5867 individual cells for the *tnaC*, *pykF*, *ptsG*, *lon*, *ompC*, and *aceB* reporter strains, respectively).

we simultaneously measured the corresponding GFP fluorescence for each bacterium (Figure 1C) and calculated the average GFP fluorescence for each strain after 17 h of growth in LB medium from biological triplicates. We found that the average percentage of cells displaying detectable aggregates strongly correlated with the average GFP fluorescence of each fluorescent strain after 17 h of growth in LB medium (Figure 1E, r Pearson coefficient of 0.94, **). For example, the reporter strain for *aceB* displayed an average GFP fluorescence 14 times higher than *tnaC*, and correspondingly a percentage of aggregate-containing bacteria 3 times higher than *tnaC*.

Aggregate-Containing Cells Downregulate GFP Expression. Next, we set out to further investigate the subpopulations of aggregate-containing bacteria for each fluorescent reporter strain. First, we investigated the distribution and intensity of GFP fluorescence in both aggregate-containing bacteria and bacteria without microscopically visible aggregates across all six fluorescent reporter strains investigated. A previous study suggested that the self-aggregating tendency of fluorescent fusion proteins can lead to an overestimation of the natural protein aggregates present inside the cell.[20] In contrast, we found that in our study the GFP signal was uniformly distributed across the whole cell area and did not colocalize with the cell regions occupied by protein aggregates in the corresponding brightfield images (Figure 1B and C). This suggests that although increasing demand for heterologous protein expression favors protein aggregation (Figure 1E), the GFP version employed in our study does not accumulate within microscopically visible protein aggregates to a different extent than the rest of the cell. Furthermore, we found that in stationary phase (i.e., after 17 h of growth in LB medium) aggregate-containing bacteria displayed a significantly lower GFP fluorescence compared to bacteria without detectable aggregates across all the investigated strains (Figure 2). This suggests that the formation of aggregates, stimulated by the demand of production of exogeneous protein, favors the entrance of aggregate-containing bacteria in a dormant or low metabolically active state. In fact, aggregate-containing bacteria downregulate the expression of all the six genes investigated in our study, including genes involved in bacterial metabolism, and reduce further production of exogenous GFP.

The Presence of Protein Aggregates Correlates with Survival to Antibiotic Treatment. Dormancy and low metabolic activity have often been associated with the persister[1] and viable but nonculturable phenotypes.[2] Therefore, we investigated whether aggregate-containing bacteria within the fluorescent reporter strain populations could survive antibiotic treatment better than bacteria that did not display protein aggregates. In order to do this, after adding to the mother machine each reporter strain in stationary phase and imaging protein aggregates as reported above, we dosed the bacteria with an antibiotic (ampicillin, gentamicin, or

https://doi.org/10.1021/acsinfecdis.1c00154
ACS Infect. Dis. XXXX, XXX, XXX−XXX

ciprofloxacin) at 25 × MIC. We found that a 3 h antibiotic treatment was sufficient to reach the second phase of the typical biphasic persister curve (Figure S2) in accordance with previous findings.[42] Therefore, after 3 h antibiotic treatment we removed the drug from the microfluidic environment and continuously supplied the bacteria with LB medium for 21 h while imaging and tracking each individual bacterium throughout the assay. Therefore, at the end of the assay we were able to identify susceptible cells that either lysed or stained with propidium iodide (Figure 3A) and persisters that survived antibiotic treatment and regrew after drug removal (Figure 3B). We were also able to identify viable but nonculturable (VBNC) cells that did not lyse and did not stain with propidium iodide but did not divide within the time frame of our assay (Figure 3C). It is worth acknowledging that previous studies found that bacteria that do not lyse and do not stain with propidium iodide could be dead.[5,43] However, this is unlikely in our assay since the bacteria that we classified as VBNC were still expressing GFP after the antibiotic was removed at t = 3h and after 21 h exposure to LB as shown in the representative images in Figure 3C (mean GFP fluorescence of 150 ± 21 a.u., 95 ± 17 a.u., and 165 ± 23 a.u. at t = 0, 3, and 24 h, respectively; N = 47 VBNC cells) and in accordance with our previous study.[8] Nevertheless, it is also conceivable that these cells could start dividing if exposed to nutrients for longer periods of time.[5,33]

By imaging and tracking 11,830 individual bacteria of the *aceB* reporter strain throughout antibiotic treatment and regrowth, we found that only 2.4%, 4.3%, and 2.5% of the bacteria that were susceptible to ampicillin, ciprofloxacin, or gentamicin treatment, respectively, contained detectable protein aggregates before antibiotic exposure (Figure 3D). In contrast, 37.7%, 57.1%, and 65.0% of the bacteria that were persistent to ampicillin, ciprofloxacin, or gentamicin treatment, respectively, contained detectable protein aggregates before antibiotic exposure (Figure 3D). Finally, 81.3%, 86.7%, and 85.0% of the bacteria that were viable but nonculturable after ampicillin, ciprofloxacin, or gentamicin treatment, respectively, contained detectable protein aggregates before antibiotic exposure (Figure 3D).

Moreover, by imaging and tracking 40,774 individual bacteria of the six investigated reporter strains throughout 3 h ampicillin treatment and 21 h regrowth in LB, we found that on average the ampicillin susceptible subpopulation contained 2.3% of bacteria with detectable aggregates before antibiotic exposure (Figure 3E). In contrast, on average, 47.5% and 70.3% of ampicillin persister and viable but nonculturable subpopulations, respectively, contained detectable aggregates before antibiotic exposure (Figure 3E). Taken together, these data corroborate the hypothesis that the presence of protein aggregates can be used as a predictor for the fate of a cell under antibiotic treatment and demonstrate that viable but nonculturable cells contain more protein aggregates than persister and susceptible cells.

Heterologous Protein Expression Favors the Formation of Persister and Viable but Nonculturable Bacteria. Next, we set out to determine whether the amount of heterologous protein expressed by bacteria increases the percentage of persister and viable but nonculturable cells within the populations of fluorescent reporter strains. Therefore, for each strain we enumerated bacteria belonging to the susceptible, persister, or viable but nonculturable phenotype. We found a significant positive correlation between the average GFP fluorescence measured across all the bacteria in each strain before antibiotic treatment, and both the percentage of persister and viable but nonculturable cells after treatment with ampicillin at 25 × MIC (r Pearson coefficient of 0.83 and 0.86, respectively, * Figure 4A and B). Furthermore, when we used a

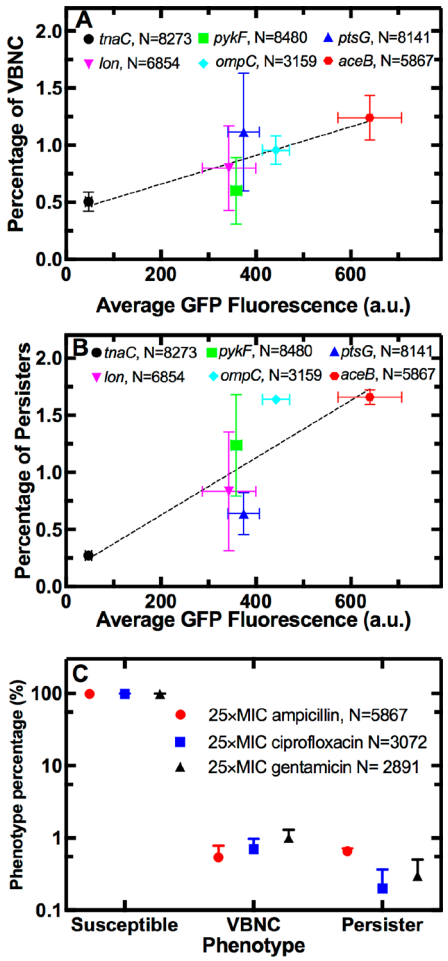

Figure 4. Heterologous protein expression favors the formation of persister and viable but nonculturable bacteria. Percentage of (A) viable but nonculturable and (B) persister *E. coli* after treatment with ampicillin at 25 × its minimum inhibitory concentration as a function of GFP fluorescence averaged over N individual bacteria before antibiotic treatment for each strain. Symbols and error bars are the mean and standard error of the mean of thousands of single-cell measurements performed in biological triplicate. N = 8273, 8480, 8141, 6854, 3159, and 5867 individual cells for the *tnaC* (hexagons), *pykF* (squares), *ptsG* (upward triangles), *lon* (downward triangles), *ompC* (diamonds), and *aceB* (circles) strain. (C) Percentage of susceptible, persister, or viable but nonculturable cells for the *aceB* reporter strain after treatment with ampicillin (circles), ciprofloxacin (squares), or gentamicin (triangles) at 25 × their minimum inhibitory concentration. Symbols and error bars are the mean and standard error of the mean of thousands of single-cell measurements performed in biological triplicate (N = 5867, 3072, and 2891 for ampicillin, ciprofloxacin, and gentamicin treatment, respectively).

Δ*dnaK E. coli* strain lacking the molecular chaperone DnaK that participates in protein disaggregation in cooperation with IbpAB and ClpB,[16] we found a significantly lower percentage of bacteria susceptible to ampicillin and a significantly higher viable but nonculturable cells compared to the *E. coli* BW25113 parental strain (** and *, respectively, Figure S3).

https://doi.org/10.1021/acsinfecdis.1c00154
ACS Infect. Dis. XXXX, XXX, XXX−XXX

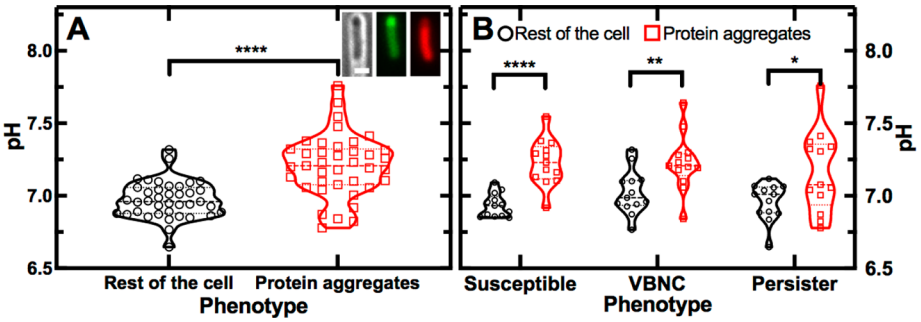

Figure 5. Protein aggregates are more basic than the rest of the cell. (A) Intracellular pH within protein aggregates (red squares) and the rest of the cell (black circles). Each data point is a pH measurement within an individual stationary phase *E. coli* bacterium carrying a pHluorin-mCherry fusion on a low copy plasmid. Data are collated on $N = 39$ bacteria from biological triplicate. Insets: brightfield, pHluorin, and mCherry fluorescence images from left to right, respectively. Scale bar: 1 μm. (B) Intracellular pH within protein aggregates (red squares) and the rest of the cell (black circles) before antibiotic treatment in cells that are then susceptible, viable, but nonculturable or persister after treatment with ampicillin at 25× of its minimum inhibitory concentration. * p-value <0.05; ** p-value <0.01; **** p-value <0.0001.

Finally, for the fluorescent strain for *aceB*, that displayed the highest percentage of persister and viable but nonculturable cells, we verified that treatment with ampicillin, ciprofloxacin, or gentamicin at 25 × MIC returned a similar percentage of persister and viable but nonculturable cells (Figure 4C). Taken together, these data demonstrate that the amount of stress caused by overexpression of heterologous proteins simultaneously increases the percentage of persisters, in accordance with a previous study,[44] and viable but nonculturable cells as well as the percentage of bacteria displaying visible protein aggregates.

Protein Aggregates Are More Basic than the Rest of the Cell. It has recently been suggested that the formation of protein aggregates in yeast is accompanied by changes in intracellular pH.[45] Therefore, we set out to investigate whether within aggregate-containing cells, aggregates are characterized by a different pH compared to the rest of the cell before antibiotic treatment. We investigated intracellular pH by using the microfluidics-based single-cell microscopy approach described above and pHluorin (Methods and ref 46), which is a pH-sensitive GFP encoded on a plasmid and reporting pH changes at the single-cell and subcellular level. We simultaneously measured the pHluorin fused mCherry fluorescence to allow for normalization of any variation in protein expression and plasmid copy number.[47] Importantly, the signals from GFP and mCherry were detected from across the whole cell area in our fluorescence images (Figure 1C and inset in Figure 5A, respectively). This suggests that these fluorescent proteins could reach and penetrate protein aggregates. Therefore, any change in pHluorin signal between the protein aggregates and the rest of the cell was due to changes in pH between these different regions within each bacterium. Interestingly, we found that before antibiotic treatment within aggregate-containing bacteria protein aggregates displayed a significantly higher pH compared to the rest of the cell (Figure 5A). Furthermore, the whole cell intracellular pH was in the range between 6.7 and 7.8 (with a mean and standard deviation of 7.1 ± 0.2) in accordance with recent work using the same pH reporter strain.[47] Moreover, when we treated these bacteria with ampicillin at 25 × its minimum inhibitory concentration we found that, before antibiotic treatment, protein aggregates were consistently and significantly more basic than the rest of the cell for all three phenotypes investigated (i.e., susceptible, VBNC, and persister; ****, **, and *, respectively, Figure 5B). Taken together, these data suggest that protein aggregates within *E. coli* are more basic compared to the rest of the cell and corroborate previous findings that changes in pH might contribute to the formation of protein aggregates.[45]

DISCUSSION

Protein aggregates within individual bacteria have often been investigated using fluorescence microscopy and reporter strains for molecular chaperones.[20,23,25] Such fluorescent strains facilitate the visualization of protein aggregates, since fluorescently labeled chaperones accumulate to a significantly greater extent within protein aggregates compared to the rest of the cell.[23,25] However, this enforced heterologous protein expression could further contribute to the accumulation of protein aggregates due to (i) the self-aggregating tendency of some fluorescent fusion proteins[20] or (ii) the burden imposed on the bacteria by the demand of producing exogenous proteins.[22] Considering that recent evidence has highlighted that protein aggregates play an important role for the outcome of antibiotic treatment,[6,16,17] here we set out to address the issues above using GFP reporter strains in combination with microfluidics-based single-cell bright-field microscopy.

First, we show that GFP does not accumulate in protein aggregates to a greater extent than the rest of the cell, thus ruling out the possibility that protein aggregates form due to the self-aggregating tendency of the fluorescent protein.

We also demonstrate that heterologous GFP expression favors the formation of protein aggregates that are instead not detectable in a stationary-phase *E. coli* culture in the absence of heterologous GFP expression. These data suggest the hypothesis that the burden imposed on the bacteria by the demand of producing exogenous proteins triggers protein aggregation in some cells within the population. In fact, the protein control system in such cells, including their chaperones and proteases, might become overloaded due to overproduction of exogenous proteins and the formation of protein aggregates. This hypothesis is further corroborated by a strong correlation between the percentage of aggregate-containing cells within the population and the average expression of heterologous GFP. Taken together, these data highlight the need for developing and using label-free techniques for investigating the formation of protein aggregates in individual bacteria. In fact, to the best of our knowledge only two papers have reported observing aggregates in *E. coli* cells in the absence of fluorescence probes to facilitate aggregate visualization.[25,48] Coquel et al. observed protein aggregates via

https://doi.org/10.1021/acsinfecdis.1c00154
ACS Infect. Dis. XXXX, XXX, XXX−XXX

bright-field microscopy in bacteria cultured for 32 h under physical confinement,[25] whereas Carrio et al. detected protein aggregates in a strain of *E. coli* with a deletion mutation for the protease La, this reducing proteolytic activity.[48] Together with these previous findings, our data suggest that intracellular or environmental stresses are a prerequisite for the formation of microscopically visible protein aggregates.

Second, we showed that aggregate-containing bacteria displayed a significantly lower GFP fluorescence compared to bacteria without visible aggregates across all the investigated strains. These data corroborate previous evidence that, in the presence of intracellular or environmental stress, aggregate-containing bacteria are characterized by reduced metabolic activity and increased dormancy depth,[6,16,17] whereas at high densities, protein aggregates can also indicate cell death.[28] Furthermore, we demonstrate that the presence of protein aggregates favors survival to antibiotic treatment. In fact, we found that only 2.4%, 4.3%, and 2.5% of the bacteria that were susceptible to ampicillin, ciprofloxacin, or gentamicin treatment, respectively, contained detectable protein aggregates before antibiotic exposure. In contrast, 37.7%, 57.1%, and 65.0% of the bacteria that were persister to ampicillin, ciprofloxacin, or gentamicin treatment, respectively, contained detectable protein aggregates before antibiotic exposure; whereas 81.3%, 86.7%, and 85.0% of the bacteria that were viable but nonculturable after ampicillin, ciprofloxacin, or gentamicin treatment, respectively, contained detectable protein aggregates before antibiotic exposure. Taken together, these data corroborate recent evidence suggesting a link between protein aggregates and bacterial dormancy, which in its turn favors survival to antibiotics,[6] as well as previous findings demonstrating that bacterial persistence increases in populations of stressed cells.[44] Here, we further deepen our understanding of this important link by demonstrating that increasing the amount of heterologous GFP expression increases the percentage of both persister and viable but nonculturable cells within a clonal *E. coli* population, as well as increasing the percentage of aggregate-containing bacteria. However, further studies need to be carried out to establish whether the accumulation of protein aggregates actually causes the formation of persister and VBNC cells.

Finally, our data suggest that within aggregate-containing bacteria protein aggregates are more basic than the rest of the cell before antibiotic treatment in cells that are then viable but nonculturable or persister after treatment with ampicillin. These data corroborate recent evidence suggesting that environmentally driven changes in intracellular pH might play a role in protein aggregation,[42] whereas their eventual role in the formation of viable but nonculturable and persister bacteria remains to be investigated, highlighting the need for further investigations of intracellular pH regulation during antibiotic treatment.

CONCLUSIONS

Protein aggregates are ubiquitous across the tree of life and the presence of aggregate-containing cells within bacterial populations might prevent effective antibiotic treatment. Here, we show that intracellular stress, caused by an increased demand for producing exogenous proteins, favors the formation of protein aggregates within stationary-phase *E. coli* and increases the percentage of persister and viable but nonculturable cells after treatment with antibiotics with different modes of action. Persister and viable but nonculturable bacteria downregulate the expression of exogenous proteins and are more likely to contain protein aggregates, although it remains to be established whether such aggregates actually cause the formation of persister and viable but nonculturable bacteria. Finally, our data suggest that such aggregates are more basic with respect to the rest of the cell. Taken together, these findings deepen our understanding of the nature and function of protein aggregates and highlight the need for developing therapies that modulate protein aggregation and pH regulation as an alternative route for the eradication of persister and viable but nonculturable cells.

METHODS

Bacterial Strains and Cultures. The parental strain *E. coli* BW25113 and the Δ*dnaK* single-deletion mutant strain lacking the molecular chaperone DnaK were purchased from Dharmacon (GE Healthcare). Fluorescent reporter strains for the following promoters *tnaC*, *pykF*, *ptsG*, *lon*, *aceB*, or *ompC* from an *E. coli* MG1655 transcriptional reporter library[31] were also purchased from Dharmacon (GE Healthcare). Each of the reporter strains has a bright, fast-folding green fluorescent protein fused to a full-length copy of an *E. coli* promoter (either *tnaC*, *pykF*, *ptsG*, *lon*, *aceB*, or *ompC*) in a low-copy plasmid (pMS201). The plasmids were extracted and transformed into the chemically competent *E. coli* BW25113 strain. Overnight cultures were prepared by picking a single colony of each *E. coli* BW25113 strain from a streak plate and growing it in 200 mL fresh LB medium (10 g/L tryptone, 5 g/L yeast extract, and 10 g/L NaCl, Melford) on a shaking incubator at 200 rpm at 37 °C for 17 h. For pH assays, *E. coli* BW25113 harboring a pBAD TOPO-mCherry-pHluorin vector (Invitrogen)[47] were kindly provided by the Summers group, Cambridge. Cultures were grown as above but with additional chloramphenicol (25 μg/mL) supplementation for plasmid maintenance and arabinose (5 μg/mL) to induce the pBAD promoter.

Minimum Inhibitory Concentration Determination. The minimum inhibitory concentration (MIC) of the employed antibiotics against *E. coli* BW25113 was determined using a 96-well plate method. *E. coli* was grown for 17 h in LB containing different concentrations of ampicillin (0.5−512 μg mL^{-1}), ciprofloxacin (0.0625−64 μg mL^{-1}), or gentamicin (0.125−128 μg mL^{-1}), and the OD595 was measured after 17 h. The MICs were measured as the lowest concentrations at which the optical density at 595 nm was the same as the control (bacteria-free LB) and were determined as 5, 4, and 0.125 μg mL^{-1} for ampicillin, gentamicin, and ciprofloxacin, respectively.

Time-Killing Assay. An *E. coli* BW25113 overnight culture grown on a shaking incubator at 200 rpm at 37 °C for 17 h was diluted 1:1000 in 20 mL LB in a 200 mL flask and cultured on a shaking incubator at 200 rpm at 37 °C for 3 h to reach exponential phase. 1 mL aliquots were withdrawn and challenged by adding ampicillin, ciprofloxacin, or gentamicin at 25 × their minimum inhibitory concentration and incubated on a shaking incubator at 200 rpm at 37 °C for 4 h. Samples were withdrawn every 30 min and diluted, and 10 μL samples were spotted on an LB agar plate for determination of colony-forming units.

Microfluidic Device Fabrication. The original mold of the mother machine microfluidic device was kindly provided by S. Jun,[34] whereas a detailed methodology for replicating and handling this device has been reported elsewhere.[8,49] Briefly,

https://doi.org/10.1021/acsinfecdis.1c00154
ACS Infect. Dis. XXXX, XXX, XXX−XXX

each microfluidic device was made by pouring a 9:1 (base:curing agent) polydimethylsiloxane (PDMS, Dow Corning) mixture onto the mold and curing it at 70 °C for 2 h. The PDMS was then peeled from the mold, access holes for the fluidic tubing were punched and the PDMS chip was then irreversibly bonded to a glass coverslip as previously reported.[50] To prevent cell adhesion to the device surfaces, 2 μL of a 50 mg/mL bovine serum albumin (BSA) solution was injected into the device and the device was incubated for 1 h at 37 °C.

Microfluidics-Based Single-Cell Microscopy for Aggregate and Antibiotic Response Phenotyping. An overnight culture was grown as described above. 10 mL of this overnight culture was centrifuged in a falcon tube (10 min at 3000 × *g* and 20 °C). The supernatant was filtered twice (Medical Millex-GS Filter, 0.22 μm, Millipore Corp.) to extract spent LB. This spent LB was then used to resuspend the bacteria to an optical density of 50 at 595 nm. This highly concentrated bacterial suspension was then injected into the BSA functionalized microfluidic device and incubated at 37 °C for approximately 20 min or until the bacteria had sufficiently (approximately 2 bacteria per channel) entered the side channels. Fluorinated ethylene propylene tubing (1/32"_0.0008") was connected to the prepunched inlet and outlet holes of the device and connected to a flow-rate measuring device (Flow Unit S, Fluigent, Paris, France) and a waste collection cylinder, respectively. At the end of the incubation period, the device was mounted onto an inverted microscope (IX73 Olympus, Tokyo, Japan); the flow rate pump was controlled using MAESFLO software (Fluigent) and spent LB used to wash excess bacteria from the main channel using spent LB at 300 μL/h for 8 min. During this time window, the initial bright field and fluorescence images were acquired for between 50 and 67 imaging areas (each area containing 23 lateral channels each hosting between one and three bacteria) of the microfluidic device, in order to image approximately 2000 bacteria per experiment. All images were acquired using a 60×, 1.2 N.A. objective (UPLSAPO60XW, Olympus) and a sCMOS camera (Zyla 4.2, Andor, Belfast, UK). For the acquisition of fluorescence images the bacteria were exposed to the blue excitation band of a broad-spectrum LED (CoolLED pE300white, Andover, UK). The light intensity and exposure time were adjusted in order to maximize the signal-to-noise ratio; FITC filter with LED light intensity set at 20% and exposure of 0.03 s for *tnaC, pykF*, and *aceB*; 20% and 0.05 s for *ptsG* and *ompC*; and 60% and 0.05 s exposure for *lon*.

After acquiring the initial images, spent LB was changed to fresh LB containing ampicillin, ciprofloxacin, or gentamicin at 25 × MIC and flowed through at 300 μL/h for 8 min before being reduced to 100 μL/h for 3 h, with images being taken hourly. After 3 h, the medium was changed again to fresh LB medium and images continued to be taken on an hourly basis for a further 3 h. As a result, during the first day of the assay, images were acquired prior to antibiotic exposure, for 3 h during exposure to antibiotics and then for 3 h after exposure. This allowed us to determine the phenotype of each cell in response to antibiotics and then extract its initial level of fluorescence. The chip was left overnight, with fresh LB continuing flowing at 50 μL/h, and a set of images acquired the next morning after 21 h of total regrowth in LB after antibiotic treatment. Finally, propidium iodide (PI, Thermo Fisher Scientific) was used to perform live/dead staining and one last set of images acquired in bright field and fluorescence using the TRITC filter (100% green LED intensity and 0.01 s exposure). The entire assay was carried out at 37 °C in an environmental chamber surrounding the microscope.

Intracellular pH Determination. In order to measure the pH of each individual cell, we used arabinose to constitutively express a fused fluorescent protein in a parental strain harboring pBAD TOPO-mCherry-pHluorin vector. As the expression of mCherry can be used to normalize by copy number, the ratio between the pH-sensitive GFP (pHluorin) and mCherry can then be used to determine intracellular pH.[47] We applied the previously described microfluidic assay to identify persister and VBNC cells prior to antibiotic exposure on this pH reporter strain. Once we determined each cell's phenotype in response to antibiotic, we then extracted the GFP/mCherry fluorescence ratio. These ratios could then be converted to a pH value based on a known standard curve.

Briefly, we exposed the pH reporter strain to 50 μM carbonyl cyanide *m*-chlorophenyl hydrazone (CCCP) at 300 μL/h for 8 min and then at 100 μL/h for 20 min. The exposure to CCCP results in disruption of the cellular membrane and allows the intracellular pH to equalize to the pH of the medium. We then flowed PBS with differing pH levels (pH 6.5, 7.0, 7.5, and 8.0, respectively) through the device one at a time at 300 μL/h for 8 min and then 100 μL/h for 20 min. We acquired images of mCherry (TRITC filter, 5% green LED intensity, and 0.03 s exposure) and GFP (FITC filter, 20% LED intensity, and 0.03 s exposure) at each pH and extracted the fluorescence intensity (see Image and Data Analysis section below). The ratio of GFP to mCherry could then be determined for each cell and the mean ratio used to generate a standard curve when plotted against the known pH.

Image and Data Analysis. Image analysis was performed using our custom Python module (*MMHelper*) to extract cellular fluorescence intensities.[51] All data reported in GraphPad Prism 7 represent mean and standard error of the mean of at least biological triplicates.

Aggregates were clearly visible in our microfluidics-based single-cell microscopy images acquired in bright field. However, in order to ensure there was no human bias we randomly selected representative bacteria that we had scored by eye as containing at least one or more visible aggregates and representative bacteria that we scored by eye as not containing a visible aggregate for each strain. We then investigated the bright field pixel intensity for the cell profiles to quantitatively validate that the phenotypes of these cells were correctly identified. Briefly, using ImageJ we drew a 5-pixel-wide line along the length of the bacterium and extracted the brightness profile. As the aggregates are primarily located at the poles, we then took the 10 most central pixels for each bacterium and used the average grayscale value to estimate a baseline value. This baseline was then subtracted and, as aggregates are visible as dark foci with lower pixel intensities, the brightness determined as the sum of at least three consecutive negative values. This allowed for the exclusion of the center of the bacterium as well as any spurious signal (less than 3 consecutive negative or positive values).[29,52] The results showed that for all cells scored as containing aggregates a trough in cumulative pixel intensity was visible across all strains, whereas the cumulative intensity for cells without aggregates remained constant throughout the cell profile.

Statistical Analysis. Statistical significance was tested using GraphPad Prism 7 by either a paired or an unpaired *t* test

https://doi.org/10.1021/acsinfecdis.1c00154
ACS Infect. Dis. XXXX, XXX, XXX−XXX

with Welch's correction depending on the specific comparison. Pearson's correlation, where r signifies the linear dependence of the variables (between −1 and 1), was used to investigate the relationship between different variables. In all statisctical analyses, $p \leq 0.05$ is indicated as *, $p \leq 0.01$ is indicated as **, $p \leq 0.001$ is indicated as ***, and $p \leq 0.0001$ is indicated as ****.

■ ASSOCIATED CONTENT

Supporting Information

The Supporting Information is available free of charge at https://pubs.acs.org/doi/10.1021/acsinfecdis.1c00154.

Quantitative comparison of the frequencies of aggregate containing bacteria in the parental strain *E. coli* BW25113 and in a Δ*dnaK* single-deletion mutant (Figure S1); time dependent killing of the parental strain *E. coli* BW25113 by ampicillin, ciprofloxacin, and gentamicin (Figure S2); the percentage of cells that are susceptible, viable but nonculturable, or persister to ampicillin treatment for the parental strain *E. coli* BW25113 and in a Δ*dnaK* single-deletion mutant (Figure S3) (PDF)

■ AUTHOR INFORMATION

Corresponding Author

Stefano Pagliara − *Living Systems Institute and Biosciences, University of Exeter, EX4 4QD Exeter, United Kingdom;* orcid.org/0000-0001-9796-1956; Email: s.pagliara@exeter.ac.uk

Authors

Olivia Goode − *Living Systems Institute and Biosciences, University of Exeter, EX4 4QD Exeter, United Kingdom*

Ashley Smith − *Living Systems Institute and Biosciences, University of Exeter, EX4 4QD Exeter, United Kingdom*

Urszula Łapińska − *Living Systems Institute and Biosciences, University of Exeter, EX4 4QD Exeter, United Kingdom;* orcid.org/0000-0003-3593-9248

Rosemary Bamford − *Living Systems Institute and Biosciences, University of Exeter, EX4 4QD Exeter, United Kingdom*

Zehra Kahveci − *Living Systems Institute and Biosciences, University of Exeter, EX4 4QD Exeter, United Kingdom;* orcid.org/0000-0001-7931-8027

Georgina Glover − *Living Systems Institute and Biosciences, University of Exeter, EX4 4QD Exeter, United Kingdom*

Erin Attrill − *Living Systems Institute and Biosciences, University of Exeter, EX4 4QD Exeter, United Kingdom*

Alice Carr − *Living Systems Institute and Biosciences, University of Exeter, EX4 4QD Exeter, United Kingdom*

Jeremy Metz − *Living Systems Institute and Biosciences, University of Exeter, EX4 4QD Exeter, United Kingdom*

Complete contact information is available at: https://pubs.acs.org/10.1021/acsinfecdis.1c00154

Author Contributions

#O.G. and A.S. contributed equally to this manuscript. S.P. designed the research and developed the project. O.G., A.S., U.L., R.B., Z.K., G.G., E.A., and A.C. performed the experiments; O.G., A.S., U.L., and S.P. analyzed the data; A.S. and J.M. wrote the image analysis code; O.G., A.S., and S.P. wrote the paper.

Funding

This work was supported by a Royal Society Research Grant (RG180007) and a Marie Skłodowska-Curie grant (H2020-MSCA-ITN-2015−675752) awarded to S.P. O.G. acknowledges support from the University of Exeter and DSTL for funding through a studentship. A.S. acknowledges support from the BBSRC through a SWBio-DTP studentship (BB/M009122/1). U.L. acknowledges support from the MRC through a Proximity to Discovery EXCITEME2 grant (MCPC17189). Z.K. acknowledges The Gordon and Betty Moore Foundation for their support (GBMF5514). E.A. acknowledges the MRC and DSTL for their support through a studentship (MR/P016162/1). G.G. was supported by an EPSRC DTP PhD studentship (EP/M506527/1).

Notes

The authors declare no competing financial interest.

■ ACKNOWLEDGMENTS

We would like to acknowledge Dr D. Summers for providing the pH reporter strain used in this investigation.

■ REFERENCES

(1) Hobby, G. L., Meyer, K., and Chaffee, E. (1942) Observations on the Mechanism of Action of Penicillin. *Exp. Biol. Med. 50*, 281−285.

(2) Xu, H.-S., Roberts, N., Singleton, F. L., Attwell, R. W., Grimes, D. J., and Colwell, R. R. (1982) Survival and Viability of Nonculturable *Escherichia Coli* and *Vibrio Cholerae* in the Estuarine and Marine Environment. *Microb. Ecol. 8*, 313−323.

(3) Li, L., Mendis, N., Trigui, H., Oliver, J. D., and Faucher, S. P. (2014) The Importance of the Viable but Non-Culturable State in Human Bacterial Pathogens. *Front. Microbiol. 5*, 258.

(4) Pinto, D., Almeida, V., Almeida Santos, M., and Chambel, L. M. M. (2011) Resuscitation of *Escherichia Coli* VBNC Cells Depends on a Variety of Environmental or Chemical Stimuli. *J. Appl. Microbiol. 110*, 1601−1611.

(5) Kim, J. S., Chowdhury, N., Yamasaki, R., and Wood, T. K. (2018) Viable but Non-Culturable and Persistence Describe the Same Bacterial Stress State. *Environ. Microbiol. 20*, 2038−2048.

(6) Dewachter, L., Bollen, C., Wilmaerts, D., Louwagie, E., Herpels, P., Matthay, P., Khodaparast, L., Khodaparast, L., Rousseau, F., Schymkowitz, J., and Michiels, J. (2021) The Dynamic Transition of Persistence towards the VBNC State during Stationary Phase Is Driven by Protein Aggregation. *bioRxiv*, 1 DOI: 10.1101/2021.02.15.431274.

(7) Ayrapetyan, M., Williams, T. C., and Oliver, J. D. (2015) Bridging the Gap between Viable but Non-Culturable and Antibiotic Persistent Bacteria. *Trends Microbiol. 23*, 7−13.

(8) Bamford, R. A., Smith, A., Metz, J., Glover, G., Titball, R. W., and Pagliara, S. (2017) Investigating the Physiology of Viable but Non-Culturable Bacteria by Microfluidics and Time-Lapse Microscopy. *BMC Biol. 15*, 121.

(9) Mulcahy, L. R., Burns, J. L., Lory, S., and Lewis, K. (2010) Emergence of *Pseudomonas Aeruginosa* Strains Producing High Levels of Persister Cells in Patients with Cystic Fibrosis. *J. Bacteriol. 192*, 6191−6199.

(10) Van den Bergh, B., Michiels, J. E., Wenseleers, T., Windels, E. M., Boer, P., Vanden, Kestemont, D., De Meester, L., Verstrepen, K. J., Verstraeten, N., Fauvart, M., and Michiels, J. (2016) Frequency of Antibiotic Application Drives Rapid Evolutionary Adaptation of *Escherichia Coli* Persistence. *Nat. Microbiol. 1*, 16020.

(11) Balaban, N. Q., Helaine, S., Camilli, A., Collins, J. J., Ghigo, J.-M., Hardt, W.-D., Harms, A., and Heinemann, M. (2019) Definitions and Guidelines for Research on Antibiotic Persistence. *Nat. Rev. Microbiol. 17*, 441.

(12) Balaban, N. Q., Merrin, J., Chait, R., Kowalik, L., and Leibler, S. (2004) Bacterial Persistence as a Phenotypic Switch. *Science 305* (5690), 1622−1625.
(13) Song, S., and Wood, T. K. (2020) PpGpp Ribosome Dimerization Model for Bacterial Persister Formation and Resuscitation. *Biochem. Biophys. Res. Commun. 523*, 281−286.
(14) Lewis, K. (2010) Persister Cells. *Annu. Rev. Microbiol. 64*, 357−372.
(15) Pu, Y., Zhao, Z., Li, Y., Zou, J., Ma, Q., Zhao, Y., Ke, Y., Zhu, Y., Chen, H., Baker, M. A. B., Ge, H., Sun, Y., Xie, X. S., and Bai, F. (2016) Enhanced Efflux Activity Facilitates Drug Tolerance in Dormant Bacterial Cells. *Mol. Cell 62*, 284−294.
(16) Leszczynska, D., Matuszewska, E., Kuczynska-Wisnik, D., Furmanek-Blaszk, B., and Laskowska, E. (2013) The Formation of Persister Cells in Stationary-Phase Cultures of *Escherichia Coli* Is Associated with the Aggregation of Endogenous Proteins. *PLoS One 8*, e54737.
(17) Yu, J., Liu, Y., Yin, H., and Chang, Z. (2019) Regrowth-Delay Body as a Bacterial Subcellular Structure Marking Multidrug-Tolerant Persisters. *Cell Discovery 5*, 1 DOI: 10.1038/s41421-019-0080-3.
(18) Schramm, F. D., Schroeder, K., and Jonas, K. (2020) Protein Aggregation in Bacteria. *FEMS Microbiol. Rev. 44*, 54−72.
(19) Mortier, J., Tadesse, W., Govers, S. K., and Aertsen, A. (2019) Stress-Induced Protein Aggregates Shape Population Heterogeneity in Bacteria. In *Current Genetics*, pp 865−869, Springer, Berlin Heidelberg. DOI: 10.1007/s00294-019-00947-1.
(20) Govers, S. K., Mortier, J., Adam, A., and Aertsen, A. (2018) Protein Aggregates Encode Epigenetic Memory of Stressful Encounters in Individual *Escherichia Coli* Cells. *PLoS Biol. 16*, No. e2003853.
(21) Weids, A. J., Ibstedt, S., Tamás, M. J., and Grant, C. M. (2016) Distinct Stress Conditions Result in Aggregation of Proteins with Similar Properties. *Sci. Rep. 6*, 24554.
(22) Bednarska, N. G., Schymkowitz, J., Rousseau, F., and Van Eldere, J. (2013) Protein Aggregation in Bacteria: The Thin Boundary between Functionality and Toxicity. *Microbiology (London, U. K.) 159*, 1795−1806.
(23) Lindner, A. B., Madden, R., Demarez, A., Stewart, E. J., and Taddei, F. (2008) Asymmetric Segregation of Protein Aggregates Is Associated with Cellular Aging and Rejuvenation. *Proc. Natl. Acad. Sci. U. S. A. 105* (8), 3076−3081.
(24) Winkler, J., Seybert, A., König, L., Pruggnaller, S., Haselmann, U., Sourjik, V., Weiss, M., Frangakis, A. S., Mogk, A., and Bukau, B. (2010) Quantitative and Spatio-Temporal Features of Protein Aggregation in *Escherichia Coli* and Consequences on Protein Quality Control and Cellular Ageing. *EMBO J. 29*, 910−923.
(25) Coquel, A., Jacob, J., Primet, M., Demarez, A., Dimiccoli, M., Julou, T., Moisan, L., Lindner, A. B., and Berry, H. (2013) Localization of Protein Aggregation in *Escherichia Coli* Is Governed by Diffusion and Nucleoid Macromolecular Crowding Effect. *PLoS Comput. Biol. 9*, No. e1003038.
(26) Merino, N., Toledo-Arana, A., Vergara-Irigaray, M., Valle, J., Solano, C., Calvo, E., Lopez, J. A., Foster, T. J., Penadés, J. R., and Lasa, I. (2009) Protein A-Mediated Multicellular Behavior in *Staphylococcus Aureus*. *J. Bacteriol. 191*, 832−843.
(27) Stöver, A. G., and Driks, A. (1999) Secretion, Localization, and Antibacterial Activity of TasA, a *Bacillus Subtilis* Spore-Associated Protein. *J. Bacteriol. 181*, 1664−1672.
(28) Baquero, F., and Levin, B. R. (2021) Proximate and Ultimate Causes of the Bactericidal Action of Antibiotics. *Nat. Rev. Microbiol. 19*, 123−132.
(29) Lapinska, U., Glover, G., Capilla-lasheras, P., Young, A. J., and Pagliara, S. (2019) Bacterial Ageing in the Absence of External Stressors. *Philos. Trans. R. Soc., B 374*, 20180442.
(30) Cama, J., Voliotis, M., Metz, J., Smith, A., Iannucci, J., Keyser, U. F., Tsaneva-Atanasova, K., and Pagliara, S. (2020) Single-Cell Microfluidics Facilitates the Rapid Quantification of Antibiotic Accumulation in Gram-Negative Bacteria. *Lab Chip 20*, 2765−2775.
(31) Zaslaver, A., Bren, A., Ronen, M., Itzkovitz, S., Kikoin, I., Shavit, S., Liebermeister, W., Surette, M. G., and Alon, U. (2006) A Comprehensive Library of Fluorescent Transcriptional Reporters for *Escherichia Coli*. *Nat. Methods 3*, 623−628.
(32) Smith, A., Kaczmar, A., Bamford, R. A., Smith, C., Frustaci, S., Kovacs-Simon, A., O'Neill, P., Moore, K., Paszkiewicz, K., Titball, R. W., and Pagliara, S. (2018) The Culture Environment Influences Both Gene Regulation and Phenotypic Heterogeneity in *Escherichia Coli*. *Front. Microbiol. 9*, 1739.
(33) Kim, J. S., Yamasaki, R., Song, S., Zhang, W., and Wood, T. K. (2018) Single Cell Observations Show Persister Cells Wake Based on Ribosome Content. *Environ. Microbiol. 20*, 2085−2098.
(34) Wang, P., Robert, L., Pelletier, J., Dang, W. L., Taddei, F., Wright, A., and Jun, S. (2010) Robust Growth of *Escherichia Coli*. *Curr. Biol. 20*, 1099−1103.
(35) Vega, N. M., Allison, K. R., Khalil, A. S., and Collins, J. J. (2012) Signaling-Mediated Bacterial Persister Formation. *Nat. Chem. Biol. 8*, 431−433.
(36) Vega, N. M., Allison, K. R., Samuels, A. N., Klempner, M. S., and Collins, J. J. (2013) Salmonella Typhimurium Intercepts *Escherichia Coli* Signaling to Enhance Antibiotic Tolerance. *Proc. Natl. Acad. Sci. U. S. A. 110* (35), 14420−14425.
(37) Hu, Y., Kwan, B. W., Osbourne, D. O., Benedik, M. J., and Wood, T. K. (2015) Toxin YafQ Increases Persister Cell Formation by Reducing Indole Signalling. *Environ. Microbiol. 17*, 1275−1285.
(38) Kotte, O., Volkmer, B., Radzikowski, J. L., and Heinemann, M. (2014) Phenotypic Bistability in *Escherichia Coli*'s Central Carbon Metabolism. *Mol. Syst. Biol. 10*, 736.
(39) Nikolic, N., Barner, T., and Ackermann, M. (2013) Analysis of Fluorescent Reporters Indicates Heterogeneity in Glucose Uptake and Utilization in Clonal Bacterial Populations. *BMC Microbiol. 13*, 258.
(40) Wood, T. K. (2016) Combatting Bacterial Persister Cells. *Biotechnol. Bioeng. 113*, 476−483.
(41) Ziervogel, B. K., and Roux, B. (2013) The Binding of Antibiotics in OmpF Porin. *Structure 21*, 76−87.
(42) Keren, I., Kaldalu, N., Spoering, A., Wang, Y., and Lewis, K. (2004) Persister Cells and Tolerance to Antimicrobials. *FEMS Microbiol. Lett. 230*, 13−18.
(43) Song, S., and Wood, T. K. (2021) Viable But Non-Culturable Cells " Are Dead. *Environ. Microbiol.*, 0−2.
(44) Hong, S. H., Wang, X., O'Connor, H. F., Benedik, M. J., and Wood, T. K. (2012) Bacterial Persistence Increases as Environmental Fitness Decreases. *Microb. Biotechnol. 5*, 509−522.
(45) Munder, M. C., Midtvedt, D., Franzmann, T., Nüske, E., Otto, O., Herbig, M., Ulbricht, E., Müller, P., Taubenberger, A., Maharana, S., Malinovska, L., Richter, D., Guck, J., Zaburdaev, V., and Alberti, S. (2016) A PH-Driven Transition of the Cytoplasm from a Fluid- to a Solid-like State Promotes Entry into Dormancy. *eLife 5*, 1−30.
(46) Miesenböck, G., De Angelis, D. A., and Rothman, J. E. (1998) Visualizing Secretion and Synaptic Transmission with PH-Sensitive Green Fluorescent Proteins. *Nature 394*, 192−195.
(47) Zarkan, A., Caño-Muñiz, S., Zhu, J., Al Nahas, K., Cama, J., Keyser, U. F., and Summers, D. K. (2019) Indole Pulse Signalling Regulates the Cytoplasmic PH of *E. Coli* in a Memory-Like Manner. *Sci. Rep. 9*, 3868.
(48) Carrió, M. M., Corchero, J. L., and Villaverde, A. (1998) Dynamics of in Vivo Protein Aggregation: Building Inclusion Bodies in Recombinant Bacteria. *FEMS Microbiol. Lett. 169*, 9−15.
(49) Cama, J., and Pagliara, S. (2021) Microfluidic Single-Cell Phenotyping of the Activity of Peptide-Based Antimicrobials. In *Polypeptide Materials: Methods and Protocols. Methods in Molecular Biology*, pp 237−253, Vol. *2208*, Humana, New York. DOI: 10.2307/j.ctt1ffjgqc.20.
(50) Pagliara, S., Chimerel, C., Langford, R., Aarts, D. G. a L., and Keyser, U. F. (2011) Parallel Sub-Micrometre Channels with Different Dimensions for Laser Scattering Detection. *Lab Chip 11*, 3365−3368.

https://doi.org/10.1021/acsinfecdis.1c00154
ACS Infect. Dis. XXXX, XXX, XXX−XXX

(51) Smith, A., Metz, J., and Pagliara, S. (2019) MMHelper: An Automated Framework for the Analysis of Microscopy Images Acquired with the Mother Machine. *Sci. Rep. 9*, 10123.
(52) Dettmer, S. L., Keyser, U. F., and Pagliara, S. (2014) Local Characterization of Hindered Brownian Motion by Using Digital Video Microscopy and 3D Particle Tracking. *Rev. Sci. Instrum. 85*, No. 023708.

https://doi.org/10.1021/acsinfecdis.1c00154
ACS Infect. Dis. XXXX, XXX, XXX−XXX